

Thallium-201 Versus Technetium-99m-MIBI SPECT in Evaluation of Childhood Brain Tumors: A Within-Subject Comparison

Lorcan A. O'Tuama, S. Ted Treves, Jerry N. Larar, Alan B. Packard, Arden J. Kwan, Patrick D. Barnes, R. Michael Scott, Peter McL. Black, Joseph R. Madsen, Liliana C. Goumnerova, Stephen E. Sallan and Nancy J. Tarbell

Departments of Radiology (Division of Nuclear Medicine), Neurology, Neurosurgery, Hematology/Oncology and Radiation Therapy, Children's Hospital and Harvard Medical School, Boston, Massachusetts

We previously found that ^{201}Tl SPECT is a highly specific agent for detection of metabolic activity of childhood brain tumors. To compare the relative diagnostic accuracy of ^{201}Tl and a technetium-based tumor-avid agent, we have obtained SPECT in 19 children using ^{201}Tl (37–111 MBq) followed immediately by $^{99\text{m}}\text{Tc}$ -methoxyisobutylisonitrile (MIBI) (370–740 MBq) intravenously. Moderate to intense focal uptake of both tracers characterized true positive cases ($n = 6$). Lesion boundaries were better defined by MIBI. Uptake of MIBI by choroid plexus occurred despite pretreatment with potassium perchlorate (6 mg/kg) and complicated interpretation of deep/paraventricular lesions. Preliminary assessment indicated sensitivity ~67% (Tl and MIBI); specificity ~91% (Tl); ~100% (MIBI). Two tumors (medulloblastoma, dysgerminoma) were Tl/MIBI nonavid. Semi-quantitative assessment of tracer uptake was made using a ratio of radioactivity in tumor-containing areas compared to uninvolved brain. Ratio values were (mean \pm s.d.) 7.88 ± 7.70 (Tl) and 27.1 ± 36.41 (MIBI). The spectrum of tumor avidity is similar for Tl and MIBI. Clearer identification of boundaries by MIBI may be an advantage in applications, e.g., radiotherapy port planning.

J Nucl Med 1993; 34:1045–1051

Continued advances in treatment of childhood brain tumors (1,2) emphasize the need for an effective method to evaluate functional activity of the disease and to allow accurate mapping of treatment response. Tumor recurrence and focal cerebral necrosis cannot be differentiated by computed tomography or magnetic resonance imaging (3–5). Diagnostic ambiguity in this situation can seriously impact on treatment planning strategies. In 28 children with recurrent brain tumor, we found ^{201}Tl SPECT to show high avidity for a wide histologic range of neoplasms. A clearer indication of the functional state of the tumor after treatment was sometimes obtained with ^{201}Tl SPECT than

with computed tomography (CT) or magnetic resonance imaging (MRI) (6).

Physical properties of technetium, such as the 140 keV gamma-ray energy and higher photon flux, are superior to thallium. Furthermore, a $^{99\text{m}}\text{Tc}$ based radiopharmaceutical offers the practical advantages of a continuously available kit-based agent. A long-term aim of our laboratory is to develop a $^{99\text{m}}\text{Tc}$ -labeled, tumor-avid radiopharmaceutical. In pursuit of this objective, we noticed that the compound hexakis (2-methoxyisobutylisonitrile)technetium(I) (MIBI) shared two properties strikingly similar to thallium: (a) It is an excellent myocardial perfusion agent (7) and (b) It is almost totally excluded by the normal blood-brain barrier. In addition, MIBI has been noted to be concentrated by other human tumors (8,9).

In view of these close similarities to thallium, we decided to evaluate the hypothesis that MIBI might share another property of thallium, viz., avidity for human brain tumors. In a preliminary study (10), we found that MIBI concentrated strongly at the site of a recurrent cerebellar astrocytoma and paralleled thallium uptake in the same lesion.

The aim of the present study was to compare the relative effectiveness of MIBI and thallium SPECT for detection of metabolic activity in a series of children with recurrent brain tumor. In addition, we wanted to compare the relative diagnostic specificity of SPECT versus MR and CT.

MATERIALS AND METHODS

Patient Population

Nineteen children (1.0 to 18.6 yr) with brain tumors diagnosed on clinical or histological grounds were studied by SPECT (Table 1). Tumor types confirmed histologically are indicated in Table 1. Sixteen patients were studied after primary treatment of their lesion.

Patients were classified as having an "active" or "inactive" tumor at the time of their imaging study. A patient was considered to have an "active" tumor when: (1) serial neurologic examinations indicated a trend of worsening referable to the site of the lesion; (2) CT/MR showed progression of a focal mass with coarse contrast or gadolinium enhancement; or (3) recent histology con-

Received Aug. 28, 1992; revision accepted Mar. 30, 1993.

For correspondence or reprints contact: L.A. O'Tuama, MD, Department of Radiology (Nuclear Medicine), Children's Hospital, 300 Longwood Ave., Boston, MA 02115.

TABLE 1
Thallium-201/^{99m}Tc-MIBI SPECT in Childhood Brain Tumors: Clinical Data and Diagnostic Imaging Results

Patient no.	Clinical data	MR/CT	²⁰¹ Tl	^{99m} Tc-MIBI	Histology	Outcome	Classification
1	Partial removal of tumor (9) followed by radiotherapy with second surgery	MR: Mass, right cerebellum. Recurrence vs. treatment effect	Intense increase right cerebellum, parietal lobe	Similar*	Astrocytoma	Not available	TP
2	Tumor resection (17), chemotherapy and radiotherapy	MR (+) [†] : Left posterior temporal mass. I: Recurrence vs. treatment effect	Intense uptake at lesion site	Similar, more intense laterally	Ependymoma, anaplastic	Surgery confirmed recurrent tumor at primary site	TP
3	Seizures 10.5 yr after primary resection, then radiotherapy	Not obtained	Normal	Normal	Medulloblastoma	No new deficit; continued seizures	TN
4	Increasing brainstem/cerebellar mass (4) attributed to recurrent tumor	MR (+): Probably progressive posterior fossa mass (+). I: Increasing tumor activity	Intense uptake, right cerebellum	Similar	Astrocytoma, grade 2	Surgery confirmed recurrence; died 14 mo after SPECT	TP
5	Resection of recurrent tumor	CT: left temporal-thalamic-midbrain, enhancing low density. I: recurrence	Moderate uptake at tumor site	Similar, less intense	Astrocytoma, grade 2	Partial removal of recurrent tumor (6 days)	TP
6	Recurrent tumor (3); radiotherapy and chemotherapy (3)	MR (+): Pons medulla mass [†] , hypo-intense centrally. I: recurrence vs. treatment effect	Intense uptake at lesion site	Similar, less extensive	Astrocytoma, high-grade	Expired with recurrence, one year after SPECT	TP
7	Radiotherapy for left frontoparietal tumor	MR: Huge mixed intensity fronto-temporal [†] mass (1)	Marked uptake, left frontoparietal lobe	Less intense, more extensive temporally	Glioblastoma multiforme	Cyst drainage 6 wk after SPECT with CT evidence of progression	TP
8	MR abnormality 1 mo after onset of seizures	R. medial temporal T1 lesion, consistent with low-grade tumor (1)	Normal	Normal	No tumor	Medial temporal sclerosis confirmed operatively	TN
9	Developed ataxia after primary diagnosis (10), radio/chemotherapy	MR: Cerebellar Hemisphere enlargement. I: tumor seeding	Normal	Normal	No recurrent tumor (eliosis on cerebellar biopsy)	Clinically stable 6 mo after SPECT	TN
10	Increasing neurologic deficit (3)	MR: Increasing brainstem mass. I: radiation injury vs. recurrence	Normal	Normal	Brainstem glioma	MR progression of mass 2 mo, clinical status improved 4 mo after SPECT	?
11	Subtotal resection (3)	MR: Residual occipital tumor consistent with stable disease	Normal	Normal	PNET	Stable areas of gadolinium-enhancing mass on MR	TN
12	Partial resection (8), craniospinal irradiation	MR: Questionable para-4th ventricular/cerebellar enhancement. I: No evidence of tumor	Normal	Normal	Medulloblastoma	MR 3 mo after SPECT showed massive craniospinal dissemination	TN
13	Posterior fossa disease (6), then chemo/radiotherapy	MR (+): Cerebellar brainstem mass [†] . I: Tumor	Normal	Normal	Medulloblastoma	Autopsy showed diffuse dissemination	FN

TABLE 1
Continued

Patient no.	Clinical data	MR/CT	²⁰¹ Tl	^{99m} Tc-MIBI	Histology	Outcome	Classification
14	Diagnosis (11) then radiotherapy	MR: Diffuse suprainfratentorial lesions. I: Residual tumor with radiation effect	Normal	Normal	Glioma	Stable CT findings 2 mo after SPECT	TN
15	Surgery (1 wk) showed residual tumor	MR: L. cerebellum, R. temporal mass [†] . I: stable disease	Mild uptake, anterior brainstem	Normal	Medulloblastoma	Received radiotherapy and chemotherapy, followed by neurologic worsening	FP (Tl); TN (MIBI)
16	Optic atrophy, decreased growth	MR: Large intra/suprasellar mixed intensity mass. I: tumor	Normal	Normal	Teratoma	Suprasellar biopsy at time of SPECT showed no active disease	TN
17	Pontine and temporal lobe lesions, 6 yr after chemo- and radiotherapy for acute lymphatic leukemia	MR: (1) Left mid-brain-pontine high-intensity lesion, low intensity rim. (2) White matter lesions. I: radiation effect	Normal	Normal	No brain tumor	Stable to improving MR on follow-up. Impression: Probable radiation effect	TN
18	Primary diagnosis (3 yr), then radiotherapy	MR (+): Mildly progressive suprasellar mass	Normal	Normal	Glioma, thalamic	Questionable recurrence 9 mo after SPECT	TN
19	Suprachiasmatic mass, nonprogressive	MR (+): Mixed intensity hypothalamic mass [†] . I: tumor	Normal	Normal	Germinoma	Clinically stable	FN

*Abnormal MIBI uptakes are compared with that of thallium.
[†]Gadolinium-enhancing.
 Numbers in parentheses indicate time interval in months before SPECT.
 TP, FP, TN, FN indicate, respectively, true-positive, false-positive, true-negative and false-negative; I = interpretation.

firmed tumor growth within the distribution of the abnormal area defined by CT/MR. Conversely, a patient was considered to have an "inactive" tumor when: (1) neurologic and CT/MR abnormalities appeared stable or improved or (2) recent histological sampling was consistent with complete removal.

SPECT Methods

Images were acquired on a rotating gamma camera (Orbiter; Siemens Medical Systems, Inc., Hoffman Estates, IL), equipped with a 30° slant-hole collimator (transaxial resolution (full width at half maximum) measured to be 14 mm) using the same basic protocol as previously described from our laboratory (6). Six patients (nos. 2, 3, 11, 12, 13, 15) received sedation consisting of 0.07 ml/kg of an institution-specific formulation administered intramuscularly (solution composition per milliliter: meperidine 25 mg, chlorpromazine 6.25 mg and promethazine 6.25 mg). One child also received 25–50 mg/kg chloral hydrate orally.

Patients were positioned using two laser beams. One beam, perpendicular to the axis of rotation of the gamma camera, aligned the lateral margin of the orbit and the external auditory meatus. The other beam, parallel to the axis of rotation, was aligned in the glabella-inion line. Image reconstruction and analysis was performed by an ADAC computer system (ADAC Laboratories, San Jose, CA) running version 4.0 (revision D) software, or by the

ICON™ Computer System (Siemens Gammasonics Inc., Hoffman Estates, IL) Chang attenuation correction was employed. Data acquisition encompassed the entire cranial neuraxial volume.

Patients received a tracer dose of thallium, 1100 μ Bq/kg, intravenously (minimum 37, maximum 111 MBq), and a SPECT study was obtained. This was followed immediately by MIBI injection (7400 μ Bq/kg, minimum 37; maximum 555 MBq) and a second SPECT acquisition. Radiation exposure to the critical organ (upper large intestine) was estimated to be 5.93 × 10⁻³ cGy per MBq.

Image Analysis

Visual Analysis. Subjective assessment of the intensity of thallium or MIBI uptake was arbitrarily scaled from 1 to 4, with 1 representing minimal uptake and 2, 3, and 4 representing mildly, moderately or markedly increased uptake, respectively.

The probability of active tumor, considering only the imaging findings, was also assessed subjectively, taking into account the location and intensity of abnormal activity. An arbitrary scale of 0 to 10 was assigned to represent the ascending likelihood of tumor activity. Uptake was considered to be positive (i.e., indicative of active disease) if average intensity ≥2 and probability ≥3.

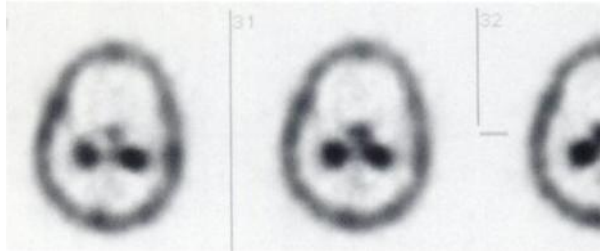


FIGURE 1. Reconstructed transaxial slices from normal brain MIBI SPECT study. Gray scale has been adjusted by lowering the upper threshold to optimize visualization of normal cerebral structures. Note minimal uptake in cerebrum and marked uptake by the normal choroid plexus.

Semiquantitative Analysis

Regions of Interest (ROIs). Operator-drawn ROIs (52–242 pixels; 7.12–33 cm²) were placed over: (a) sites with no CT or MR abnormality or (b) areas of abnormally increased MIBI and/or thallium distribution. Region boundaries were selected by two observers to conform to the site of maximum tracer uptake within the lesion. Uptake was assessed as the radioactivity ratio of ROI (b) to ROI (a).

CT and MR

The mean interval between CT or MR and SPECT studies was 12.5 ± 10.3 (range 1–23) days ($n = 17$). All images were read by the same neuroradiologist (PDB) who was blinded to the SPECT findings.

CT Methods

CT studies were done ($n = 1$) with and without contrast enhancement using the General Electric 9800 CTT system and intravenous injection of 68% ioversal media (0.5 ml/kg, maximum 100 ml). Axial 10-mm sections were obtained throughout the entire brain, often with 5-mm sections through the posterior fossa or region of interest.

MR Methods

MR images ($n = 15$) were obtained on a 1.5 Tesla GE Signa Unit (software release version 4.7). Images were acquired as 5-mm sagittal thallium sections (TR 600 msec/TE 20 msec) followed by axial proton density (TR 2000 msec/TE 30 msec) and T2 (TR 2000 msec/TE 90 msec) axial sections, often with additional coronal T1-weighted or proton density-weighted and T2-weighted sections. Subsequently, gadolinium-DTPA was injected ($n = 10$) at a rate of 0.1 ml/kg (maximum 10 ml) followed by sagittal or axial

T1-weighted sections and occasionally by coronal T1-weighted and/or axial proton density-weighted and T2-weighted images.

For Patient 3, SPECT was requested as part of a workup for seizure localization. Because there was minimal clinical suspicion of tumor recurrence, structural imaging was not obtained.

RESULTS

Thallium and MIBI SPECT

Visual Analysis. The distribution of both thallium and MIBI showed a basic similarity in that both tracers were excluded almost totally from cerebral tissues inside the normal blood-brain barrier (Fig. 1). The only distinguishing feature was the consistent and prominent uptake of MIBI by the normal choroid plexus. The tracer appeared to label both lateral and fourth ventricular choroid plexus equally and prominently. This uptake persisted even after the preadministration of potassium perchlorate (6 mg/kg orally) 30 min before administration of the tracer. Thallium uptake also occurred in the region of the choroid plexus but less distinctly than with MIBI.

True-Positive Studies ($n = 6$; Thallium and MIBI). Moderate to intense focal uptake of both tracers was noted at the site of tumor activity (Fig. 2). Because of the greater signal-to-noise ratio, MIBI more clearly defined the margins of the lesion. In most cases, the distribution of thallium and MIBI to the lesion were parallel.

Assessment of thallium uptake in the paraventricular regions was difficult because of the normal accumulation in the region of the choroid plexus. In such cases, the MIBI “map” of the plexus allowed us to assess the limits of thallium abnormality more clearly. Five of the six thallium/MIBI-avid tumors were astrocytomas. Three were infratentorial and three supratentorial.

False-Positive Studies ($n = 1$ Thallium; $n = 0$ MIBI). In a patient with treated posterior fossa medulloblastoma ($n = 15$), there was a mild and diffuse increase in the uptake of thallium in the region of the anterior part of the brainstem and within the cerebellar vermis. This observation occurred 6 days after complete resection of residual tumor. MIBI uptake was normal.

True-Negative Studies ($n = 9$ Thallium; $n = 10$ MIBI). The ten true-negative cases included astrocytomas, PNET

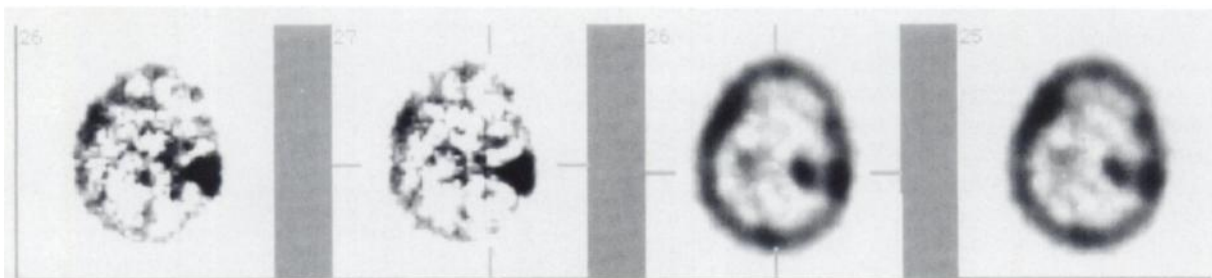


FIGURE 2. Recurrent anaplastic ependymoma (Patient 2). Reconstructed transaxial slices are shown. Superior aspect of the image corresponds to frontal region; left side of brain is to the viewer's right. Thallium (two left most) and MIBI (two right most) images are shown. Both tracers show intensely increased uptake in the region of the left posterior parietal lobe. For the MIBI image there is: (1) lower background versus thallium and (2) partial superimposition of the left lateral ventricular choroid plexus on the abnormality. Note also mild asymmetry of uptake in the region of the frontal calvarium, which is associated with previous surgery.

TABLE 2

Semi-quantitative Assessment of Thallium and MIBI Uptake by Childhood Brain Tumors: True-Positive Patients

Patient no.	Tl*	MIBI*
2	3.3	16.8
1	5.2	14.5
4	23.4	100.6
6	6.9	18.0
7	4.5	4.2
5	4.0	8.4

*Numbers refer to ratio of radioactivity of ^{201}Tl or of $^{99\text{m}}\text{Tc}$ -MIBI in regions from tumor-containing brain to regions from uninvolved cerebrum. See text for details of computation.

and medulloblastoma. Four tumors were infratentorial, four supratentorial and two had diffuse, supratentorial and infratentorial involvement.

False-Negative Studies ($n = 2$; *Thallium and MIBI*). Patient 19 had a suprachiasmatic mass initially indolent which progressed and revealed itself as a germinoma 2 mo after the SPECT. Patient 13 had a posterior fossa medulloblastoma.

Indeterminate ($n = 1$). Patient 10 presented with clinical and MR findings indeterminate for radiation effect versus recurrence and the issue remained uncertain 4 mo later.

Semi-quantitative Analysis. In the true-positive cases ($n = 6$) (Table 2), the ratio of radioactivity in tumor-containing areas to that in normal brain was 7.88 ± 7.70 (mean \pm s.d.); 3.3–23 (range) for thallium and 27.1 ± 36.4 (mean \pm s.d.); 4.2–100.6 (range) for MIBI.

Statistical Analysis

Because of the relatively small number of patients involved in this study, definitive statistical estimates of the diagnostic effectiveness of thallium and MIBI were not achievable. Preliminary assessments indicate a sensitivity of ~67% (thallium and MIBI) and a specificity of ~91% and ~100% for thallium and MIBI, respectively.

Comparison of SPECT with CT/MR Findings

True-Positive Patients. Comparison of the disease probability assessments made by SPECT and MRI showed that SPECT generally confirmed metabolically active disease within the volume of intensity abnormality depicted on MRI. In two patients, however, SPECT suggested a more homogeneous increase in metabolic activity than was appreciated from examination of the MR abnormality, which showed more regional variation.

The assessment of the extent of metabolic abnormality was different in three of the true-positive patients. MRI suggested a greater extent in two and a lesser extent in one patient.

True-Negative Patients. The SPECT scan was normal in five patients when the MR study was more equivocal.

DISCUSSION

Both tracers showed minimal uptake in normal brain, as noted previously for thallium (6), and presumably reflected almost total exclusion by the blood-brain barrier. The main difference between the tracers was the strong, selective uptake of MIBI by the choroid plexus. Potassium perchlorate is known to inhibit uptake of pertechnetate by the choroid plexus (11) but had no effect on the uptake of MIBI. This phenomenon may represent a specific choroid plexus uptake mechanism for MIBI, independent of the pertechnetate carrier. It is conceivable that a similar mechanism may be obtained for MIBI uptake by other epithelial tissues: perchlorate also failed to block isonitrite uptake by the human thyroid gland (12).

Experimental studies have suggested different underlying mechanisms for tissue accumulation of thallium and MIBI. Membrane potential and potassium permeability have been suggested to be important for thallium uptake by human brain tumors (13). Mitochondrial and plasma-membrane potentials may contribute to MIBI uptake both in human carcinoma cell lines (14) and in cultured chick myocardial cells (15).

Despite these suggested differences in uptake mechanism, the distribution of thallium and MIBI to tumors was broadly similar in the present series: both showed a relatively parallel uniform accumulation at sites of activity. Interestingly, one low-grade lesion was missed with MIBI but detected with thallium. It will be important to confirm in a larger series whether lesion characterization, including staging, can be assisted by a comparison of these two tumor-avid agents.

The "growing edge" of tumor activity was more clearly defined by MIBI than by thallium. The hypothesis that this difference might reflect a difference in tumor cell affinity for the chemical moiety of $^{99\text{m}}\text{Tc}$ -MIBI seems unlikely, since the pattern of uptake of the two radiopharmaceuticals throughout the main bulk of the tumors appeared parallel. It appears more probable that the sharper definition of the lesion edge by MIBI reflects the physical advantages of a technetium-based label, as discussed above. This property of $^{99\text{m}}\text{Tc}$ -MIBI may be of importance in applications such as stereotactic radiosurgery of brain tumors, where accurate definition of the lesion boundary is critical (16).

The normal uptake of MIBI by the choroid plexuses presents both advantages and disadvantages in assessment of tumor activity. Utilizing only MIBI, normal uptake tended to obscure lesions in the deep paraventricular regions. However, the availability of previously acquired thallium data helped to resolve this difficulty. Conversely, we had previously noted difficulty (6) in confirming the limits of abnormal thallium uptake in deep lesions because of its tendency to accumulate in the region of the plexus. In such cases, the MIBI map identified the true limits of the choroid plexus and thus clarified the thallium data.

Semi-quantitative analysis indicated thallium uptake at the site of active disease to be markedly increased, up to

more than twentyfold higher than normal brain values. With the exception of Patient 4, our present results lie within two standard deviations of our estimates of thallium uptake in a previous series (6).

The results also parallel previous experience with thallium uptake in adult brain tumors. Mean tumor-to-normal brain ratios in this series tend to be somewhat higher than those obtained by Black et al. (17) and by Kosuda et al. (18), who noted mean values of 4.7, and 2.4, respectively, for high-grade astrocytomas.

MIBI accumulation in tumor was even more strikingly elevated than in the case of thallium. In four of five patients, the degree of MIBI uptake at the tumor site exceeded, by two-fold to five-fold, that noted for thallium.

Assessment of tumor function by both thallium and MIBI compares highly favorably with data from widely used tumor-avid PET radiopharmaceuticals, such as [¹⁸F]fluorodeoxyglucose (19) and L-methyl-¹¹C-methionine (20). Representative values for radioglucose imaging of human brain tumors, expressed as a ratio of tracer utilization by the tumor to that seen in uninvolved brain, are 1.2 (19) and 1.48 (21). Comparable values in adult gliomas for L-methyl-¹¹C-methionine include ranges of 1.04–4.8 (20,23); for childhood brain tumors, 1.1–3.0 (24). Thus, using the upper range of the PET estimates, mean thallium uptake exceeds mean uptake of FDG by 4.4-fold, and of methionine by 1.64-fold. MIBI exceeds FDG by 18.3 and methionine by 5.7. For the PET studies, we recognize that the age and histologic types of tumors differed in some patients from our series. Furthermore, we did not make a within-subject comparison of MIBI and PET. Hence, our results do not allow any generic conclusion about the relative sensitivity of positron tumor-avid radiopharmaceuticals versus SPECT agents.

It is of further interest that MIBI affinity for metabolically active tumor may exceed that of another tumor-avid SPECT tracer, L-3-[¹²³I]iodo-alpha-methyl tyrosine. Bier-sack et al. have reported tumor-to-normal brain ratios with this tracer ranging from 1.4 to 2.6 (25). These values are comparable to the PET-based estimates of tumor amino acid uptake cited above. Hence, MIBI may have a greater chemical affinity than radiolabeled amino acids for certain tumors. Further evaluation of this hypothesis will require direct comparison of MIBI with L-methyl-¹¹C-methionine, L-3-[¹²³I]iodo-alpha-methyl tyrosine, or equivalent SPECT or PET-based amino acid agents.

Preliminary estimates of diagnostic accuracy are presented in the form of sensitivity and specificity analysis. We recognize that the sample number underlying these estimates is small. However, there is no reason to believe that the population studied was not normally distributed, and we believe that the analysis is valid, although the magnitude of the values may change as additional patients are studied. Sensitivity and specificity for thallium detection of childhood brain tumors was 67% and 91%, which agrees closely with our earlier estimates (6). These findings suggest that the primary role for functional brain imaging in

brain neoplasms may be to identify recurrent disease as a cause for clinical worsening when MR and/or CT or clinical evidence is equivocal.

As in our previous experience, SPECT and MRI appeared to have complementary roles in the assessment of tumor activity. In true-positive patients, SPECT added to the MR definition of “stable” residual disease information regarding functional activity. In two of the true-positive patients, this functional characterization was validated by the course. In three patients, the extent of abnormality indicated by MRI exceeded that on the functional image. It is possible that in such context the SPECT data may match more closely the true limits of tumor activity. This possibility can be assessed by newer approaches such as image fusion/registration (26). In true-negative patients, the functional image clearly allowed a truer assessment of disease activity than was obtainable by MRI.

Our system for definition of tumor activity attempted only to define this parameter *at the time of and immediately after SPECT imaging*. The activity status, as defined by our criteria, was not necessarily predictive of long-term outcome. Three of the “true-negative” patients eventually showed definite (Patients 12 and 14) or possible (Patient 18) dissemination of their disease.

The present experience reflected in all but three patients the uptake characteristics of thallium and MIBI in children presenting with the question of possibly *recurrent* tumor. It is possible that the distribution of these tracers may have different properties at the time of disease presentation, when the influence of treatment modalities can be excluded. This hypothesis remains to be evaluated by serial SPECT studies, beginning with baseline evaluation and repeated coupled to treatment cycles.

In summary, a preliminary study with 19 children indicates that MIBI, like thallium, is a highly effective agent to delineate functional activity of childhood tumor. Intratumoral distribution of thallium and MIBI is broadly similar. However, further study is needed to evaluate possible differences in tracer distribution that may have important implications for grading. Review of our experience with both thallium and MIBI indicates that both tracers complement in important ways information derived from MRI. In particular, the true functional state of residual disease may be assessed. This information has important implications for assessment of treatment response and contingent clinical decision-making in the child with brain tumor.

ACKNOWLEDGMENT

The authors thank DuPont-Merck, Inc. for the generous gift of MIBI kits.

REFERENCES

1. Allen JC, Bloom J, Ertel I, et al. Brain tumors in children: current cooperative and institutional chemotherapy trials in newly diagnosed and recurrent disease. *Semin Oncol* 1986;13:110–122.
2. Horowitz ME, Poplack DG. Development of chemotherapy treatment for pediatric brain tumors. *Neurologic Clinics* 1991;11:9:363–373.
3. Rollins N, Mendelsohn D, Mulne A, et al. Recurrent medulloblastoma:

- frequency of tumor enhancement on Gd-DTPA MR. *AJR* 1990;10:155:153-157.
4. Wilms G, Marchal G, Demaerel PH, Van Hecke P, Baert AL. Gadolinium-enhanced MRI of intracranial lesions. A review of indications and results. *Clin Imaging* 1991;15:153-165.
 5. Valk PE, Dillon WP. Diagnostic imaging of central nervous system radiation injury. In: Gutin PH, Leibel SA, Sheline GE, eds. *Radiation injury to the central nervous system*. New York: Raven Press; 1991:211-237.
 6. O'Tuama LA, Janicek M, Barnes PD, et al. Thallium-201/^{99m}Tc-HMPAO SPECT imaging of treated childhood brain tumors. *Pediatric Neurol* 1991; 11:249-257.
 7. Wackers FJTh, Berman DS, Maddahi J, et al. Technetium-99m hexakis 2-methoxyisobutyl isonitrile: human biodistribution, dosimetry, safety and preliminary comparison to thallium for myocardial perfusion imaging. *J Nucl Med* 1989;30:301-311.
 8. Briele B, Hotze A, Kropp J, et al. A comparison of ²⁰¹Tl and ^{99m}Tc-MIBI in the follow-up of undifferentiated thyroid carcinoma. *Nuklearmedizin* 1991; 30:115-124.
 9. Caner B, Kitapci M, Aras T, Erben G, Ugur O, Bekdik C. Increased accumulation of hexakis (2-methoxyisobutylisonitrile)technetium(I) in osteosarcoma and its metastatic lymph nodes. *J Nucl Med* 1991;32:1977-1978.
 10. O'Tuama LA, Packard AB, Treves ST. Case report: SPECT imaging of pediatric brain tumor with hexakis (methoxyisobutylisonitrile) technetium (I). *J Nucl Med* 1990;31:2040-2041.
 11. Kaplan WD, Macomb JG, Strand RD, Treves S. Suppression of ^{99m}Tc-pertechnetate uptake in a choroid plexus papilloma. *Radiology* 1973;109: 395-396.
 12. Civelek AC, Durski K, Shafiqe I, et al. Failure of perchlorate to inhibit Tc-99m isonitrile binding by the thyroid during myocardial perfusion studies. *Clin Nucl Med* 1991;16:358-361.
 13. Brismar T, Collins VP, Kesselberg M. Thallium uptake relates to membrane potential and potassium permeability in human glioma cells. *Brain Res* 1989;500:30-36.
 14. Delmon-Moingeon LI, Piwnica-Worms D, Van den Abbeele AD, Holman BL, Davison A, Jones AG. Uptake of the cation hexakis(2-methoxyisobutylisonitrile)-technetium-99m by human carcinoma cell lines in vitro. *Cancer Res* 1990;50:2198-2202.
 15. Piwnica-Worms D, Kronauge JF, Chiu ML. Enhancement by tetraphenylborate of technetium-99m-MIBI uptake kinetics and accumulation in cultured chick myocardial cells. *J Nucl Med* 32:12-20.
 16. Lunsford LD, Kondziolka D, Flickinger JC. Stereotactic radiosurgery: current spectrum and results. *Clin Neurosurg* 1992;38:405-444.
 17. Black KL, Hawkins RA, Kim KT, Becker DP, Lerner C, Marciano D. Use of thallium-201 SPECT to quantitate malignancy grade of gliomas. *J Neurosurg* 1989;71:342-346.
 18. Kosuda S, Shioyama Y, Kamat N, et al. Differential diagnosis between recurrence of brain tumor and radiation necrosis by ²⁰¹Tl SPECT. *Nippon Igaku Hoshasen Gakkai Zasshi—Nippon Acta Radiologica* 1991;51:415-421.
 19. DiChiro G. Positron emission tomography using [¹⁸F]fluorodeoxyglucose in brain tumors. A powerful diagnostic and prognostic tool. *Invest Radiol* 1987;22:360-371.
 20. Derlon JM, Bourdet C, Bustany P, et al. Carbon-11-L-methionine uptake in gliomas. *Neurosurgery* 1989;25:720-728.
 21. Hiesiger E, Fowler JS, Wolf AP, et al. Serial PET studies of human cerebral malignancy with [1-¹¹C]putrescine and [1-¹¹C]2-deoxy-D-glucose. *J Nucl Med* 1987;28:1251-1261.
 22. Blacklock JB, Oldfield EH, Di Chiro G, et al. Effect of barbiturate coma on glucose utilization in normal brain versus gliomas. Positron emission tomography studies. *J Neurosurg* 1987;66:71-75.
 23. Lilja A, Bergstrom K, Hartvig P, et al. Dynamic study of supratentorial gliomas with L-methyl-¹¹C-methionine and positron emission tomography. *AJNR* 1985;6:505-514.
 24. O'Tuama LA, Phillips PC, Strauss LC, et al. Two-phase [¹¹C]L-methionine PET scanning in diagnosis of childhood brain tumors. *Pediatric Neurol* 1990;6:163-170.
 25. Biersack HJ, Coenen HH, Stocklin G, et al. Imaging of brain tumors with L-3-[¹²³I]iodo-alpha-methyl tyrosine and SPECT. *J Nucl Med* 1989;30:110-112.
 26. Pellizari CA, Chen GT, Spelbring DR, Weichselbaum RR, Chen CT. Accurate three-dimensional registration of CT, PET and/or MR images of the brain. *J Comput Assist Tomogr* 1989;13:320-361.